

# Optical Properties of TiO<sub>2</sub> Suspensions: Influence of pH and Powder Concentration on Mean Particle Size

Sedat Yurdakal,<sup>†</sup> Vittorio Loddo,<sup>\*,‡</sup> Bernardí Bayarri Ferrer,<sup>§</sup> Giovanni Palmisano,<sup>‡</sup> Vincenzo Augugliaro,<sup>‡</sup> Jaime Giménez Farreras,<sup>§</sup> and Leonardo Palmisano<sup>‡</sup>

Kimya Bölümü, Fen Fakültesi, Anadolu Üniversitesi, Yunus Emre Kampüsü, 26470 Eskişehir, Turkey, "Schiavello-Grillone" Photocatalysis Group, Dipartimento di Ingegneria Chimica dei Processi e dei Materiali, Università di Palermo, Viale delle Scienze, 90128 Palermo, Italy, and Departament d'Enginyeria Química, Universitat de Barcelona, c/ Martí i Franquès, 1, 08028 Barcelona, Spain

The optical properties of photocatalytic suspensions, that is, the absorption and scattering coefficients, depend on the effective size of particle agglomerates. This work aimed to investigate if the pH and powder concentration affect the particle size and eventually the optical properties of suspensions. Aqueous suspensions of commercial TiO<sub>2</sub> powders irradiated by monochromatic light have been optically characterized by measuring the transmitted photon flow as a function of catalyst mass and by applying an asymptotic form of the Kubelka–Munk solution of the radiative transfer equation. It was found that equal masses of catalyst at different pH and concentration values show different particle size distributions and therefore different optical properties. Moreover, the quantum yield for the photocatalytic reaction of phenol was determined for each catalyst and pH.

## 1. Introduction

Heterogeneous photocatalytic processes are generally carried out by using semiconductor catalyst particles suspended in aqueous solution and irradiated by monochromatic or polychromatic light with energy that exceeds the band gap of the used material. Among the various semiconductor oxides TiO<sub>2</sub> in the anatase phase (band gap energy  $E = 3.2$  eV corresponding to 382 nm light) has been widely used<sup>1</sup> because of its high photostability, efficiency, and low cost and has proven to be able to decompose many organic and inorganic compounds to carbon dioxide, water, and mineral acids.

The basic principles of heterogeneous photocatalysis are well-established<sup>2</sup> even if, as a result of the inherent complexity of photocatalytic processes, there are still open questions concerning the role of the active species<sup>3</sup> responsible for the photocatalytic reactions (HO• radicals and/or positive holes) and whether the reaction takes place on the surface or in solution.<sup>4</sup> The applicative aspects of this technology are being also investigated with particular attention devoted to the optimization of the process operative conditions. On this ground it is necessary to know the optical properties of photocatalytic suspensions under real working conditions<sup>5–11</sup> for evaluating the energetic efficiency of different photocatalytic systems and therefore for correctly comparing them.

The catalyst particle size plays an essential role in determining the optical properties of the suspension and consequently the radiant field inside the photoreactor.<sup>7,8</sup> In water the TiO<sub>2</sub> catalyst is not dispersed as primary particles but as solid aggregates,<sup>5</sup> called secondary particles; in fact, regardless of the primary particle size, there is particle aggregation<sup>11</sup> which depends on catalyst concentration and on factors such as the charge density/potential of the particle surfaces and van der Waals forces.

Indeed the presence of small catalyst particles suspended in the liquid phase causes scattering and absorption phenomena<sup>9</sup>

whose extent depends not only on catalyst concentration<sup>10</sup> but also on physical and chemical properties of the catalyst powders. The kinetics of photocatalytic reaction is affected in a complex way both by the reactant and product concentrations and by the distribution of the radiant field inside the system,<sup>12</sup> so it may be concluded that the optical properties of the suspension eventually affects the performance of the photocatalytic process.<sup>13</sup>

To determine the optical properties of commercial polycrystalline TiO<sub>2</sub> catalysts suspended in water and irradiated by monochromatic radiation, a new approach has been applied.<sup>14–19</sup> The values of absorption and scattering coefficients are obtained by measuring the incident and transmitted photon flows, determining the transmittance of the suspension as a function of the mass of the catalyst. An approximated form of the hyperbolic solution of the radiation transfer equation obtained by Kubelka and Munk can be applied for optically thick media; this solution assumes a simple expression of the kind of Lambert–Beer law with two adjustable parameters from which the optical coefficients can be readily calculated.<sup>20</sup>

This paper aims to investigate if the pH of the solution and the amount of catalyst in the suspension may affect the mean particle size and therefore the optical properties of the suspension. Three commercial TiO<sub>2</sub> specimens have been used both for the optical characterization runs and for the reactivity runs which allowed to determine the quantum yield for the used test reaction, that is, the photocatalytic oxidation of phenol.

## 2. Experimental Section

**2.1. Materials.** The following commercial TiO<sub>2</sub> samples were used: Degussa P25 (80% anatase, 20% rutile, specific surface area, SSA, 50 m<sup>2</sup>·g<sup>-1</sup>), Merck (100% anatase, SSA 10 m<sup>2</sup>·g<sup>-1</sup>), and Tiioxide A (100% anatase, SSA 8 m<sup>2</sup>·g<sup>-1</sup>); all samples were used as received from the factory. All the chemicals used were reagent grade (Aldrich).

**2.2. Apparatus.** The experimental apparatus mainly consists of a radiation source and a photoreactor. An illuminator–collimator (Oriel Corporation, U.S.A.) equipped with a 1000 W high-pressure Hg lamp (L5173 Hanovia) and a monochro-

\* To whom corresponding should be addressed. Tel.: + 39 091 6567221. Fax: + 39 091 6567280. E-mail: loddo@dicpm.unipa.it. URL: www.dicpm.unipa.it.

<sup>†</sup> Anadolu Üniversitesi.

<sup>‡</sup> Università di Palermo.

<sup>§</sup> Universitat de Barcelona.

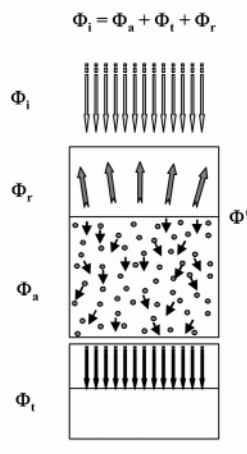
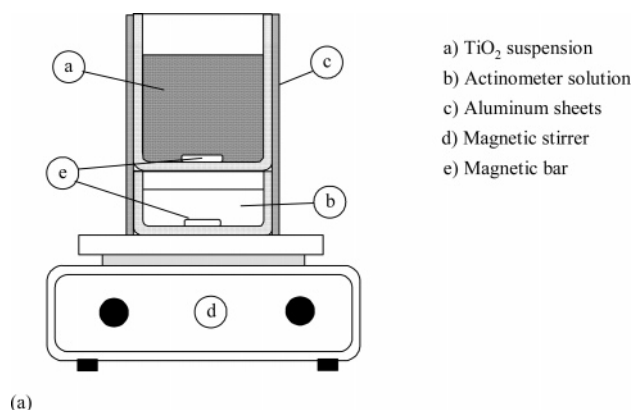


**Figure 1.** (a) Scheme of the experimental setup; (b) macroscopic photon balance on the suspension.

mator (Oriel 7240) was allowed to carry out runs at fixed wavelength ( $370$  or  $310 \pm 2$  nm). A water filter was present in the illuminator so that IR radiation was cut-off. The photoreactor, whose scheme is reported in Figure 1a, consisted of two cylindrical vessels (i.d. 58 mm) of quartz glass, vertically positioned one on the top of the other; the upper vessel contained the catalyst suspension, and the lower one contained the actinometer solution. The external surfaces of both vessels were covered by mirror-polished aluminum sheets. The suspension was directly irradiated from the circular top surface having a cross-sectional area of  $26.42 \text{ cm}^2$ .

The volume of the actinometer solution was always  $40 \text{ cm}^3$ . The suspension and the actinometer solution were mixed by using a magnetic stirrer at a constant speed of 240 rpm, which allowed the good suspension of the solid with a formation of a small whirl at the free liquid–air surface. The temperature of the whole system was about 308 K for all the experiments.

**2.3. Experiments.** For determining the particle size distribution a known amount of catalyst was suspended in  $100 \text{ cm}^3$  of water and agitated by a magnetic stirrer (240 rpm) for 20 min, and after that the sample was analyzed. It was checked that with this treatment time the size distribution of secondary particles was independent of the agitation time. For each catalyst these measurements were carried out at pH values of 2, 4, 8, 8.5, and 10 in a concentration range of  $40\text{--}200 \mu\text{g}\cdot\text{cm}^{-3}$ .

The experimental runs aimed to determine the optical properties of suspensions consisted in measuring the transmitted photon flow as a function of the catalyst mass. These runs lasted 120 s when irradiating with 370 nm light or 180 s with 310 nm light and were carried out by using suspension volumes ranging from 50 to  $240 \text{ cm}^3$ . For each experiment the same procedure

followed for determining the particle size distribution was strictly repeated: the agitation of the suspension was carried out at a constant speed of the magnetic stirrer (240 rpm) and lasted 20 min before starting the irradiation. The transmittance measurements were carried out at pH values of 3, 6.5, and 8.5 and for a particle concentration of approximately  $65 \mu\text{g}\cdot\text{cm}^{-3}$ .

A series of photoreactivity tests were carried out by using the phenol photodegradation as the test reaction. These runs lasted a maximum of 240 min and were performed under the same experimental conditions used for the transmittance measurements with a suspension volume of  $100 \text{ cm}^3$  and a catalyst amount of approximately  $65 \mu\text{g}\cdot\text{cm}^{-3}$ . The initial phenol concentration was about 0.2 mM. Suspension samples of  $4 \text{ cm}^3$  were withdrawn every approximately 30 or 60 min for analyzing; the catalyst was immediately separated from the aqueous solution by filtering through  $0.45 \mu\text{m}$  Millex Millipore filters. After each withdrawal the vessel containing the suspension was raised to maintain a constant incident photon flow.

**2.4. Analytical Methods.** The size distribution of secondary particles was measured by using a Malvern laser light scattering apparatus (model ZetaMaster).

Actinometry was used for determining the transmitted photon flow. The actinometer solution was a ferrioxalate one, appropriate for measuring the 370 or 310 nm photons.<sup>21</sup> The absorbance of the actinometer samples was measured at  $\lambda = 510 \text{ nm}$  by using a Shimadzu UV2401 spectrophotometer.

Phenol quantitative determination was carried out by means of a HPLC Beckman Coulter (System Gold 126 Solvent Module and 168 Diode Array Detector), equipped with a Luna  $5\mu$  Phenyl-Hexyl column ( $250 \text{ mm}$  long  $\times$   $2 \text{ mm}$  i.d.); the eluent consisted of methanol, acetonitrile, and a 40 mM  $\text{KH}_2\text{PO}_4$  aqueous solution with volumetric ratio of 17.5:17.5:65%, respectively. The flow rate was  $3.33 \times 10^{-3} \text{ cm}^3\cdot\text{s}^{-1}$ .

### 3. Optical Properties Determination

The optical properties of an irradiated scattering medium may be evaluated by solving the radiation transfer equation that expresses the radiation intensity balance at a fixed wavelength.<sup>7</sup> The analytical solution of this integro-differential equation is very difficult so that it is necessary to introduce some simplifying assumptions. A very easy approach is the Schuster–Schwarzschild approximation<sup>22</sup> based on the main assumptions that (i) the scattering and absorption phenomena are properties of a continuum irradiated layer;<sup>8</sup> (ii) the Lambert cosine law holds involving isotropic distribution of scattering;<sup>23</sup> (iii) the particles are randomly distributed, and their size is smaller than the thickness of the layer; and (iv) the layer is subjected to diffuse radiation. Under these statements the radiation field inside the layer is assumed to consist of two isotropic diffuse fluxes propagating in opposite directions. The intensities of  $I$  and  $J$  (the fluxes in the forward and backward directions, respectively) are coupled according to two differential equations:

$$-\frac{dI}{dx} = (k + s)I - sJ \quad (1)$$

$$+\frac{dJ}{dx} = (k + s)J - sI \quad (2)$$

in which  $x$  is the coordinate along which light propagation occurs and  $k$  and  $s$  are the absorption and scattering coefficients, respectively.

Among the several solutions proposed for these equations, the most accepted one in the field of diffuse reflectance is the

hyperbolic solution of Kubelka–Munk<sup>24</sup> which reads

$$T = \frac{(1 - R_\infty^2) \exp\left(-b \frac{2s^* m_{\text{cat}}}{A}\right)}{1 - R_\infty^2 \exp\left(-2b \frac{2s^* m_{\text{cat}}}{A}\right)} \quad (3)$$

where  $b$  is defined as

$$b = \sqrt{\left(1 + \frac{k^*}{s^*}\right)^2 - 1} \quad (4)$$

in which  $T$  is the medium transmittance (the ratio of the transmitted photon flow to the incident one),  $m_{\text{cat}}$  is the mass of catalyst,  $A$  is the cross section of photoreactor,  $s^*$  and  $k^*$  are the scattering and absorption coefficients per unit catalyst concentration, and  $R_\infty$  is the diffuse reflectance of the sample; its value is always less than the unity and depends only on the  $k^*/s^*$  ratio:

$$R_\infty = 1 + \frac{k^*}{s^*} - \sqrt{\left(\frac{k^*}{s^*}\right)^2 + 2 \frac{k^*}{s^*}} \quad (5)$$

For an optically thick participating medium,<sup>20</sup> that is, at values of  $R_\infty$  and  $m_{\text{cat}}$  for which the inequality

$$R_\infty^2 \exp\left(-2b \frac{2s^* m_{\text{cat}}}{A}\right) \ll 1 \quad (6)$$

holds, eq 3 may be approximated by the following one:

$$T = (1 - R_\infty^2) \exp\left(-b \frac{2s^* m_{\text{cat}}}{A}\right) \quad (7)$$

which indicates an exponential relationship between the transmittance and the mass of catalyst.

It was experimentally found<sup>16–19</sup> that the dependence of transmitted photon flow on mass of catalyst follows an apparent Lambert–Beer law when the mass of catalyst is higher than a threshold value:

$$\Phi_t = \Phi' \exp(-Em_{\text{cat}}) \quad (8)$$

in which  $\Phi'$  is a constant and  $E$  is the Napierian extinction coefficient.

By comparing eq 8 with eq 7, the following identities may be deduced:

$$\Phi' = \Phi_i (1 - R_\infty^2) \quad (9)$$

$$E = 2 \frac{s^*}{A} \sqrt{\left(1 + \frac{k^*}{s^*}\right)^2 - 1} \quad (10)$$

On this ground, if the inequality expressed by eq 6 is satisfied, the transmittance data may be fitted to eq 8, then allowing the determination of the values of  $\Phi'$  and  $E$  by a suitable least-squares best fitting procedure.

The  $\Phi'$  parameter of eq 8 has a physical meaning. In fact, as in the present case there is no radiation loss through the lateral wall,<sup>25</sup> a macroscopic energy balance on the total volume of the irradiated suspension (see Figure 1b) gives the following relationship:

$$\Phi_i = \Phi_r + \Phi_a + \Phi_t \quad (11)$$

in which  $\Phi_i$  is the incident photon flow,  $\Phi_r$  is the backward

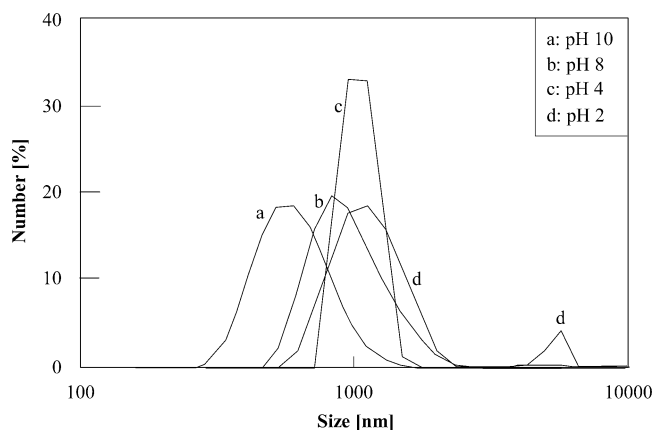


**Figure 2.** Particle size distribution at different pH value's for a TiO<sub>2</sub> Merck concentration of 65 µg·cm<sup>-3</sup>.

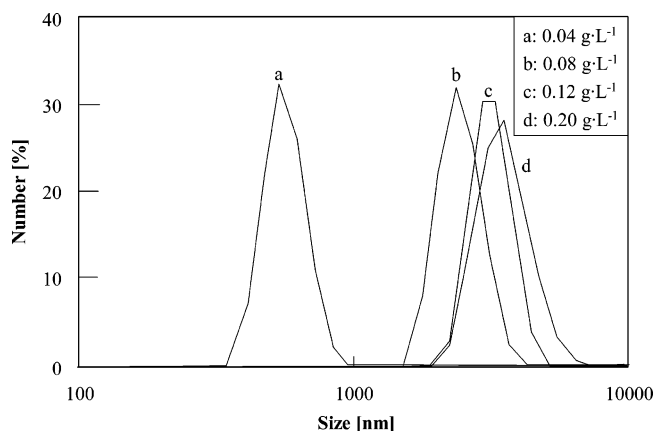


**Figure 3.** Particle size distribution for different TiO<sub>2</sub> Degussa P25 concentrations at pH 8.5.

scattered one,  $\Phi_a$  is the absorbed one, and  $\Phi_t$  is the transmitted one. This balance, by substituting eq 8 into it, allows  $\Phi'$  to be determined under the limiting condition of  $m_{\text{cat}} = 0$

$$\Phi' = \Phi_i - \Phi_r \quad (12)$$

and therefore the  $\Phi'$  parameter indicates the difference between the incident and the backward reflected photon flow, that is, the photon flow able to penetrate the suspension.

#### 4. Results and Discussion

Figures 2 and 3 report representative distribution curves of the dimensions of the aggregates at different pH values and concentrations, respectively. The general indication of the results (see Figure 2) is that the aggregate size distribution is binomially dispersed at pH 2 while it gets monodispersed at higher pH values; moreover, an increase of pH determines a shift of the distribution curve toward lower values of particle size. As far as the influence of catalyst concentration is concerned, the results indicate (see Figure 3) that the monodispersed aggregate size distribution shifts to higher values by increasing the catalyst concentration. Figures 4–6 show the mean sizes of the agglomerates for Merck, Degussa P25, and Tioxide A catalysts, respectively, as a function of catalyst concentration at different pH values. Figure 7 reports the same values plotted versus the pH for a fixed catalyst concentration. As it may be noted from these figures, the particle size increases with the catalyst concentration and generally decreases by increasing the pH. As far as Merck and Tioxide A are concerned, a slight dependence on the catalyst concentration was found with the pH being the

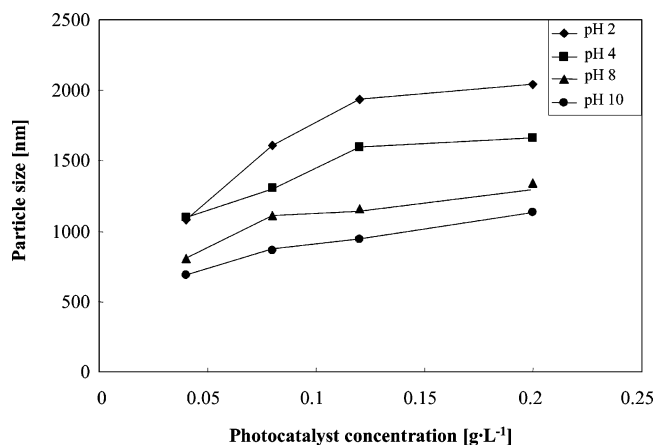


**Figure 4.** Mean particle size versus photocatalyst concentration at different pH values for TiO<sub>2</sub> Merck.

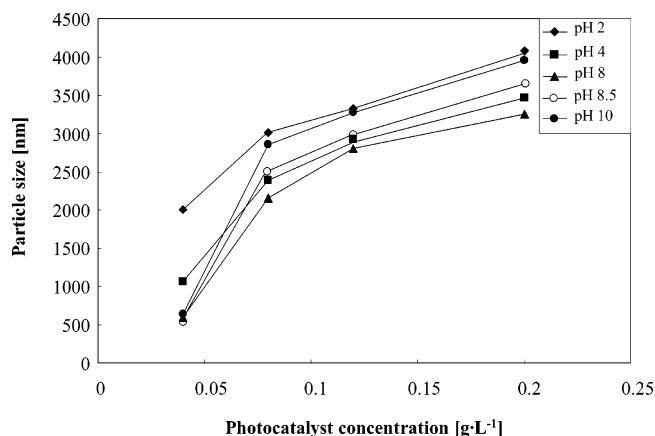


**Figure 5.** Mean particle size versus photocatalyst concentration at different pH values for TiO<sub>2</sub> Degussa P25.

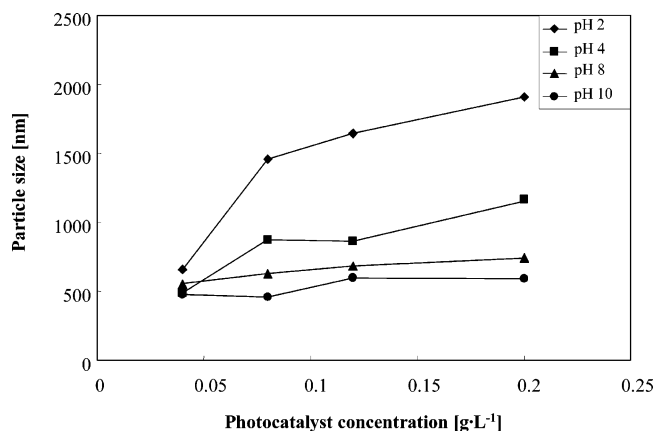


**Figure 6.** Mean particle size versus photocatalyst concentration at different pH values for TiO<sub>2</sub> Tioxide A.

most important parameter. On the contrary, Degussa P25 showed the strongest dependence on catalyst concentration while the influence of pH was less important. Moreover, it must be noted that the particle size values decrease from pH 2 to pH 8; for pH values higher than 8 they increase, and for pH 10 the values are very near to those obtained at pH 2. The different behavior among the catalysts can be due to the different allotropic phases present: only anatase for Merck and Tioxide A and anatase and rutile for Degussa P25.

The aggregation occurring in stirred suspensions of small particles is a well-known phenomenon.<sup>11,26–28</sup> It has been reported that the dynamics of aggregation<sup>26</sup> mainly depend on

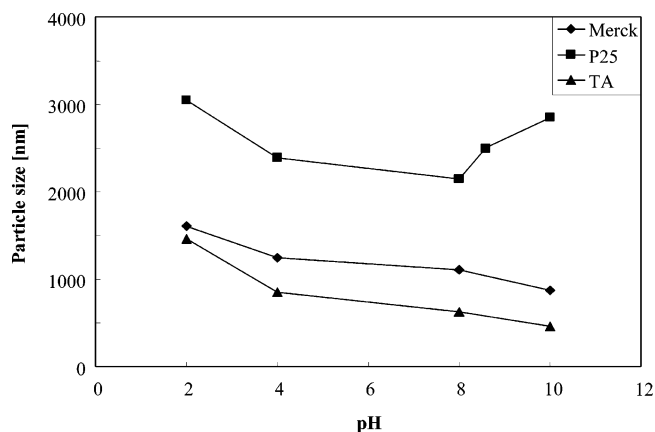


**Figure 7.** Mean particle size versus pH for a catalyst concentration of 65  $\mu\text{g}\cdot\text{cm}^{-3}$ .

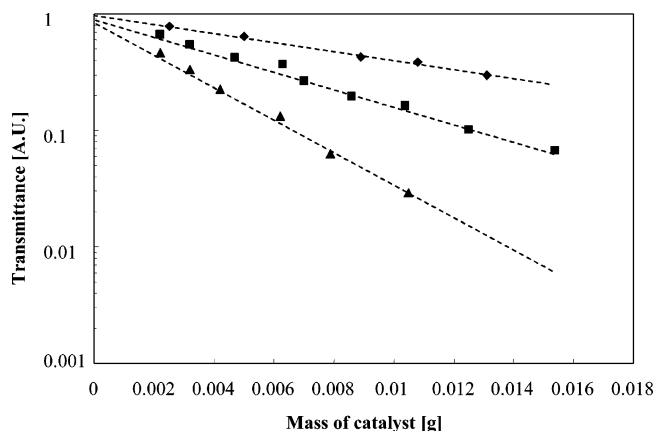


**Figure 8.** Transmittance values versus the amount of solid in the presence of 370 nm monochromatic radiation at pH 3 (◆), 6.5 (■), and 8.5 (▲) for Merck photocatalyst (constant catalyst concentration of 65  $\mu\text{g}\cdot\text{cm}^{-3}$ ). The broken lines through the data represent the phenomenological relationship (eq 8).

the particle collisions which are related to the local shear flow. In suspensions for which light backscattering can be measured, aggregation occurs under physicochemical conditions corresponding to long-range attractive forces and short-range repulsive forces. The aggregation property of the particles together with their size distributions have been also investigated by measuring the rheological properties<sup>27,28</sup> of titanium dioxide dispersions in water over a wide range of powder concentrations, temperatures, and pH values, and the same behavior here reported has been observed.

Figure 8 reports typical results of transmittance versus mass of catalyst for the different pH values used. The phenomenological equation (eq 8) was found to fit the experimental data for almost all the mass amounts used in this work, and by applying a least-squares best fitting procedure the values of  $\Phi'$  and  $E$  were determined. Table 1 reports the  $\Phi'/\Phi_i$  ratio and  $E$  figures together with  $d$ , the mean particle size, obtained under different irradiation conditions. The values of the Napierian extinction coefficient increase by decreasing the mean particle size and by increasing the radiation energy. The Degussa P25 catalyst shows the highest  $E$  values as also the strongest dependence on the wavelength. The  $E$  and  $\Phi'/\Phi_i$  figures have been used for determining the values of  $s^*$  and  $k^*$  by means of eqs 9 and 10. In fact by knowing  $\Phi'$ , eq 9 gives the  $R_\infty$  value which through eq 5 furnishes the value of the  $k^*/s^*$  ratio. By putting the known values of  $E$  and  $k^*/s^*$  in eq 10, the value of  $s^*$  and, therefore, that of  $k^*$  may be determined. The values of  $E$ ,  $s^*$ , and  $k^*$  agree very well with literature data,<sup>10,20,29,30</sup> even

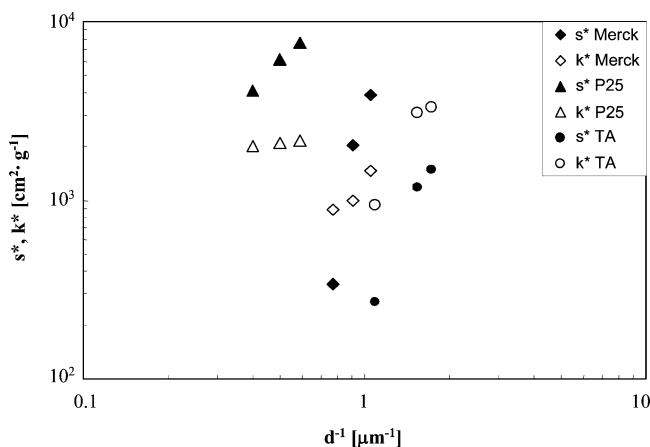
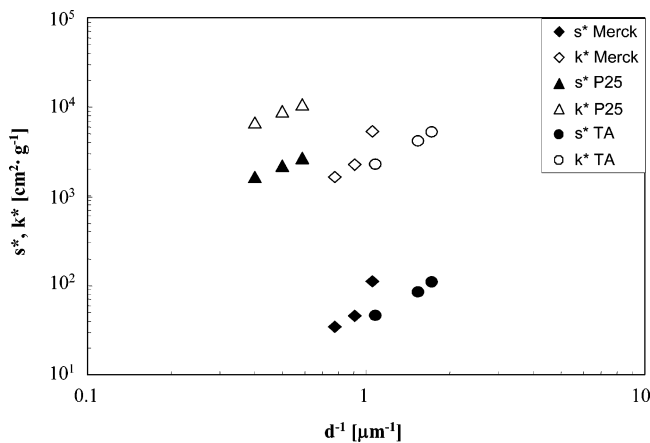
**Table 1.** Values of the Napierian Extinction Coefficient,  $E$ , of the Mean Particle Size,  $d$ , and of the  $\Phi'/\Phi_i$  Ratio at Different pH Values and Radiation Wavelengths

catalyst	pH = 3			pH = 6.5			pH = 8.5		
	$E$ [g <sup>-1</sup> ]	$d$ [μm]	$\Phi'/\Phi_i$	$E$ [g <sup>-1</sup> ]	$d$ [μm]	$\Phi'/\Phi_i$	$E$ [g <sup>-1</sup> ]	$d$ [μm]	$\Phi'/\Phi_i$
Monochromatic Radiation at 370 nm: $\Phi_i = 8.62 \times 10^{-8}$ Einstein/s									
Degussa P25	402	2.2	0.80	534	1.7	0.77	650	2.5	0.77
Merck	92	1.3	0.98	179	1.1	0.85	325	1.0	0.95
Tioxide A	87	0.9	0.98	250	0.7	0.98	327	0.6	0.6
Monochromatic Radiation at 310 nm: $\Phi_i = 3.64 \times 10^{-8}$ Einstein/s									
Degussa P25	830	2.2	0.99	1000	1.7	0.93	624	2.5	0.85
Merck	122	1.3	0.999	173	1.1	0.999	328	1.0	0.999
Tioxide A	150	0.9	0.999	311	0.7	0.999	410	0.6	0.999

if different experimental apparatuses were used for their determination.

Figures 9 and 10 show the values of  $s^*$  and  $k^*$  as function of  $1/d$  for all the catalysts at 370 and 310 nm, respectively. As reported in the pertinent literature<sup>31,32</sup> both parameters increase by decreasing the particle size showing an almost linear dependence on the  $1/d$  parameter, whereas the absorption coefficients increase by increasing the energy of the impinging radiation and the scattering coefficients generally decrease at very low values for Tioxide A and Merck samples while for Degussa P25 they remain almost constant.

The asymptotic solution of the Kubelka–Munk model is valid for describing the dependence of transmitted photon flow on the catalyst mass under the condition that the suspension is

**Figure 9.** Values of scattering ( $s^*$ ) and absorption ( $k^*$ ) coefficients as a function of mean particle size for radiation of 370 nm.**Figure 10.** Values of scattering ( $s^*$ ) and absorption ( $k^*$ ) coefficients as a function of mean particle size for radiation of 310 nm.

optically thick,<sup>20,24</sup> that is, that the strong inequality expressed by eq 6 is satisfied. This condition is safely fulfilled when the following inequality is satisfied (see eq 6):

$$m_{\text{cat}} > \frac{A}{4bs^*} R_{\infty}^2 \quad (13)$$

Introducing eqs 4 and 10 into eq 13 and rearranging results in

$$m_{\text{cat}} > \frac{1}{2E} R_{\infty}^2 \quad (14)$$

All the values of  $m_{\text{cat}}$  used for determining  $E$  and  $R_{\infty}$  satisfy the previous inequality, and thus the asymptotic solution of the Kubelka–Munk model may be considered valid in this case.

To compare the performances of different photocatalytic systems,<sup>33,34</sup> the rate of photon absorption and the intrinsic reaction rate must be determined. The knowledge of these parameters allows the quantum yield,  $\varphi$ , to be calculated for monochromatic radiation:

$$\varphi = \frac{\frac{\text{reacted molecules}}{\text{unit surface area} \cdot \text{time}}}{\frac{\text{absorbed photons}}{\text{unit surface area} \cdot \text{time}}} = \frac{\text{reacted molecules}}{\text{absorbed photons}} \quad (15)$$

For determining the  $\varphi$  values the reaction rate for phenol degradation was determined under the same irradiation conditions used for transmittance measurements.

For engineering purposes it is useful to find out a simple and easy-to-use rate equation that fits the experimental rate data. It is generally accepted<sup>4</sup> that the Langmuir–Hinshelwood (LH) model can phenomenologically represent the kinetics. In the simplest form this two-step model is based on the assumptions that (i) adsorption of reactants is a rapid equilibrium process and (ii) the slow rate-determining step involves species present in a monolayer at the solid–liquid interface. The simple rate form of the LH approach, however, may have origins which take into account different photoreaction mechanisms.<sup>35–37</sup> For photocatalytic systems where adsorption–desorption is not equilibrated, the slow step approximation cannot be applied. In this case the steady state approach<sup>38</sup> has been applied by assuming that the surface concentrations of reacting species are in the steady state. This approach leads to a kinetic expression that resembles LH kinetics but with the advantage that the model parameters explicitly depend on light intensity. In fact, experimentally observed dependences of the rate parameters of the LH model on light intensity can only be explained if the assumption of the adsorption–desorption equilibrium is relaxed.

Under the operative conditions used the rate of phenol photocatalytic degradation in oxygenated suspensions can be described by a pseudo-first-order kinetics,<sup>39–41</sup> and it can be written in terms of Langmuir–Hinshelwood kinetics as

$$r_s = -\frac{1}{S} \frac{dN}{dt} = k' \theta_{\text{PHEN}} = k' \frac{KC_{\text{PHEN}}}{1 + KC_{\text{PHEN}}} \quad (16)$$

in which  $N$  indicates the phenol moles present in the liquid phase,  $t$  indicates the reaction time,  $S$  indicates the catalyst surface area,  $k'$  indicates the surface pseudo-first-order rate constant, and  $\theta_{\text{PHEN}}$  indicates the fractional sites coverage by phenol. This last parameter is given by the Langmuir relationship which has been substituted in eq 16,  $C_{\text{PHEN}}$  being the phenol concentration in the solution and  $K$  being the adsorption equilibrium constant. By considering that the phenol concentra-

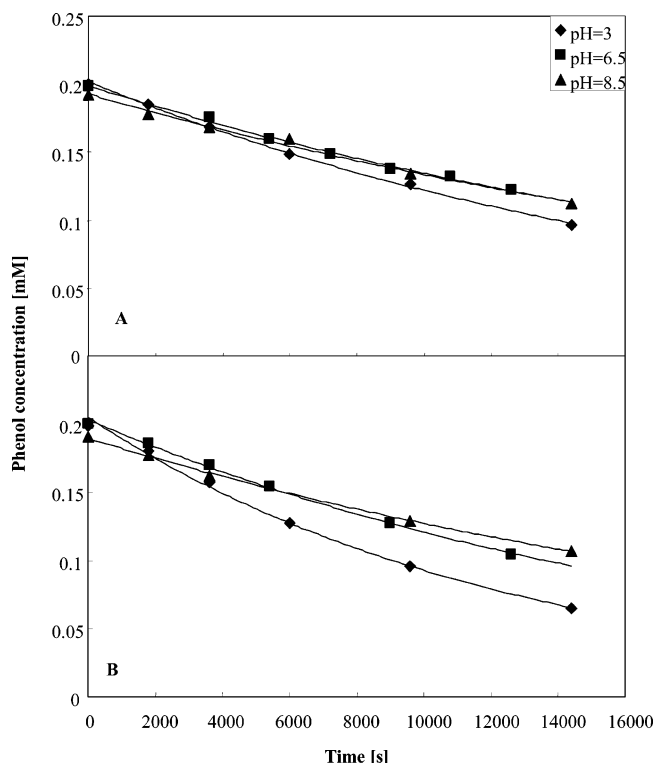


**Figure 11.** Values of phenol concentration versus irradiation time for runs carried out with TiO<sub>2</sub> Merck (65 μg·cm<sup>-3</sup>) irradiated at 310 nm (A) and 370 nm (B): pH 3 (◆); pH 6.5 (■); pH 8.5 (▲).

tion was the parameter experimentally measured, the pseudo-first-order rate equation assumes the following form:

$$r_s = -\frac{V}{S} \frac{dC_{\text{PHEN}}}{dt} = k' \frac{KC_{\text{PHEN}}}{1 + KC_{\text{PHEN}}} \quad (17)$$

The runs carried out with both monochromatic radiations indicated that the phenol degradation rate follows first-order kinetics for all of the catalysts, thus suggesting that the inequality  $KC \ll 1$  holds and therefore producing the following rate equation:  $r_s = k_{\text{obs}}C_{\text{PHEN}}$  in which the observed rate constant,  $k_{\text{obs}}$ , is equal to  $k'K$ . By integrating the first-order rate equation and by fitting the resulting exponential relationship to the experimental  $C-t$  data, the values of  $k_{\text{obs}}$  have been obtained. The continuous lines drawn in Figure 11 represent the kinetic model, which, as it may be noted, fits very well the experimental data. The large duration of the reactivity runs guaranteed a high confidence on the fitted  $k_{\text{obs}}$  values ( $R^2 > 0.98$ ). For calculating the  $\varphi$  values from eq 15, the number of phenol molecules reacted in the first 120 or 180 s (the duration times of actinometer runs carried out at 370 or 310 nm, respectively) was determined from the values of  $k_{\text{obs}}$ , and the number of absorbed photons was obtained by using eqs 11 and 12. It was confidently assumed that at the start of the photodegradation runs only phenol molecules are present in the reacting mixture so that the aliquot of absorbed photons useful for the photoreaction is utilized only for phenol degradation.

Table 2 reports the figures of the observed rate constant,  $k_{\text{obs}}$ , and of the quantum yield,  $\varphi$ , for all the catalysts under the used experimental conditions; the  $\varphi$  values are comparable with those reported in the literature.<sup>42</sup> For all the catalysts the quantum yield increases by increasing the energy of the radiation. For Merck and Tiioxide A the kinetic constant decreases probably owing to the fact that the photon intensity at 310 nm is quite less than that at 370 nm; on the contrary for Degussa P25 the

**Table 2.** Values of Quantum Yield,  $\varphi$ , and of Observed Rate Constant,  $k_{\text{obs}}$ , for the Used Photocatalysts at Different pH Values and Radiation Wavelengths

catalyst	$\varphi$ [%]			$k_{\text{obs}} \times 10^9$ [m·s <sup>-1</sup> ]		
	pH = 3	pH = 6.5	pH = 8.5	pH = 3	pH = 6.5	pH = 8.5
Monochromatic Radiation at 370 nm						
Degussa P25	2.66	1.90	2.18	2.77	1.47	2.34
Merck	2.49	1.96	1.26	12.2	8.09	6.15
Tioxide A	2.80	1.32	1.27	12.56	8.74	8.08
Monochromatic Radiation at 310 nm						
Degussa P25	5.3	5.4	5.5	3.02	2.28	2.66
Merck	2.63	2.48	2.06	7.73	5.95	5.65
Tioxide A	4.54	2.3	2.1	11.12	7.92	7.18

$k_{\text{obs}}$  values increase. Even if these catalysts show a Napierian extinction coefficient at 310 nm higher than that at 370 nm and then they absorb a greater aliquot of incident photons, the  $\varphi$  values indicate that at 310 nm a greater part of absorbed photons is useful for reaction events. As far as the influence of pH is concerned, the highest  $\varphi$  values are for pH 3, as expected.<sup>31</sup> By increasing the pH, for Merck and Tiioxide A the  $\varphi$  values decrease while for Degussa P25 at 310 nm they seem independent of the pH and at 370 nm there is a minimum both for  $\varphi$  and for  $k_{\text{obs}}$ .

The main findings of this work may be summarized as follows: (i) the optical properties of photocatalyst suspensions (Napierian extinction coefficient and absorption and scattering coefficients) depend on particle size and on radiation energy; (ii) the pH and the catalyst concentration affect the particle size; and (iii) the quantum yield of a photoreaction is a very complex function of all the previous parameters and then difficult to be foreseen.

In conclusion the performance of a photocatalytic process is strongly affected by the particle size, whose mean value depends on many factors among which are catalyst concentration and pH. Owing to the fact that the photocatalytic results obtained in slurries of particulate TiO<sub>2</sub> are sensitive to the state of dispersion of the TiO<sub>2</sub>, the particle size measurement must be carried out under the same experimental conditions used for performing the photoprocess. This conclusion is important because it affects any comparison of photoactivity of different TiO<sub>2</sub> samples when measured in a fixed reaction or of the relative activities of catalysts for two or more photoreactions.

## Acknowledgment

The authors wish to thank Tiioxide and Degussa for kindly furnishing some TiO<sub>2</sub> samples. MIUR (Rome, Italy) is gratefully acknowledged for financial support.

## Literature Cited

- (1) Fujishima, A.; Hashimoto, K.; Watanabe, T. *TiO<sub>2</sub> Photocatalysis: Fundamentals and Applications*; Bkc: Tokyo, 1999.
- (2) Schiavello, M. *Heterogeneous Photocatalysis*; John Wiley & Sons: New York, 1995.
- (3) Yang, S.; Lou, L.; Wang, K.; Chen, Y. Shift of Initial Mechanism in TiO<sub>2</sub>-Assisted Photocatalytic Process. *Appl. Catal., A* **2006**, *301*, 152.
- (4) Emeline, A. V.; Ryabchuk, V. K.; Serpone, N. Dogmas and Misconceptions in Heterogeneous Photocatalysis. Some Enlightened Reflections. *J. Phys. Chem. B* **2005**, *109*, 18515.
- (5) Alfano, O. M.; Cabrera, M. I.; Cassano, A. E. Modeling of Light Scattering in Photochemical Reactors. *Chem. Eng. Sci.* **1994**, *49*, 5327.
- (6) Pasquali, M.; Santarelli, F.; Porter, J. F.; Yue, P. L. Radiative Transfer in Photocatalytic Systems. *AIChE J.* **1996**, *42*, 532.
- (7) Romero, R. L.; Alfano, O. M.; Cassano, A. E. Cylindrical Photocatalytic Reactors. Radiation Absorption and Scattering Effects Produced by Suspended Fine Particles in an Annular Space. *Ind. Eng. Chem. Res.* **1997**, *36*, 3094.

- (8) Cassano, A. E.; Alfano, O. M. Reaction Engineering of Suspended Solid Heterogeneous Photocatalytic Reactors. *Catal. Today* **2000**, *58*, 167.
- (9) van de Hulst, H. C. *Light Scattering by Small Particles*; Dover: New York, 1981.
- (10) Yang, Q.; Ang, P. L.; Ray, M. B.; Pehkonen, S. O. Light Distribution Field in Catalyst Suspensions within an Annular Photoreactor. *Chem. Eng. Sci.* **2005**, *60*, 5255.
- (11) Pirkanniemi, K.; Sillanpaa, M. Heterogeneous Water Phase Catalysis as an Environmental Application: A Review. *Chemosphere* **2002**, *48*, 1047.
- (12) Brandi, R. J.; Alfano, O. M.; Cassano, A. E. Evaluation of Radiation Absorption in Slurry Photocatalytic Reactors. 1. Assessment of Methods in Use and New Proposal. *Environ. Sci. Technol.* **2000**, *34*, 2623.
- (13) Martin, C. A.; Camera-Roda, G.; Santarelli, F. Effective Design of Photocatalytic Reactors: Influence of Radiative Transfer on their Performance. *Catal. Today* **1999**, *48*, 307.
- (14) Augugliaro, V.; Palmisano, L.; Schiavello, M. Photon Absorption by Aqueous TiO<sub>2</sub> Dispersion Contained in a Stirred Photoreactor. *AIChE J.* **1991**, *37*, 1096.
- (15) Schiavello, M.; Augugliaro, V.; Palmisano, L. An Experimental Method for the Determination of the Photon Flow Reflected and Absorbed by Aqueous Dispersions Containing Polycrystalline Solids in Heterogeneous Photocatalysis. *J. Catal.* **1991**, *127*, 332.
- (16) Augugliaro, V.; Loddo, V.; Palmisano, L.; Schiavello, M. Performance of Heterogeneous Photocatalytic Systems: Influence of Operational Variables on Photoactivity of Aqueous Suspension of TiO<sub>2</sub>. *J. Catal.* **1995**, *153*, 32.
- (17) Augugliaro, V.; Loddo, V.; Palmisano, L.; Schiavello, M. Heterogeneous Photocatalytic Systems: Influence of Some Operational Variables on Actual Photons Absorbed by Aqueous Dispersions of TiO<sub>2</sub>. *Sol. Energy Mater. Sol. Cells* **1995**, *38*, 411.
- (18) Augugliaro, V.; Loddo, V.; Palmisano, L.; Schiavello, M. Bestimmung der Quantenausbeute von Heterogenen Photokatalytischen Systemen. Bestimmung des Absorbierten und Reflektierten Photonenflusses in Wäßrigen Suspensionen von Polykristallinem Titandioxid. In *Photochemie konzepte, methoden, experimente*; Wöhrle, D., Tausch, M. W., Stohrer, W. D., Eds.; Wiley: Weinheim, 1998; p 459.
- (19) Schiavello, M.; Augugliaro, V.; Loddo, V.; López-Muñoz, M. J.; Palmisano, L. Quantum Yield of Heterogeneous Photocatalytic Systems: Revisiting an Experimental Method for Determining the Absorbed Photon Flow. *Res. Chem. Intermed.* **1999**, *25*, 213.
- (20) Loddo, V.; Addamo, M.; Augugliaro, V.; Palmisano, L.; Schiavello, M.; Garrone, E. Optical Properties and Quantum Yield Determination in Photocatalytic Suspensions. *AIChE J.* **2006**, *52*, 2565.
- (21) Murov, S. L. *Handbook of Photochemistry*; Dekker: New York, 1973.
- (22) Modest, M. F. *Radiative Heat Transfer*; McGraw-Hill: New York, 1993.
- (23) Brandi, R. J.; Alfano, O. M.; Cassano, A. E. Rigorous Model and Experimental Verification of the Radiation Field in a Flat Solar Collector Simulator Employed for Photocatalytic Reactions. *Chem. Eng. Sci.* **1999**, *54*, 2817.
- (24) Kortüm, G. *Reflectance Spectroscopy: Principles, Methods, Applications*; Springer-Verlag: New York, 1969.
- (25) Jirkovsky, J.; Boule, P. Actinometric and Spectrophotometric Study of the Light Interaction with Aqueous Suspensions of Various Solids. *J. Photochem. Photobiol., A* **1997**, *111*, 181.
- (26) Tontrup, C.; Gruy, F.; Courmil, M. Turbulent Aggregation of Titania in Water. *J. Colloid Interface Sci.* **2000**, *229*, 511.
- (27) Yang, H.-G.; Li, C.-Z.; Gu, H.-C.; Fang, T.-N. Rheological Behavior of Titanium Dioxide Suspensions. *J. Colloid Interface Sci.* **2001**, *236*, 96.
- (28) Yaremko, Z. M.; Nikipanchuk, D. M.; Fedushinskaya, L. B.; Uspenskaya, I. G. Redispersion of Highly Disperse Powder of Titanium Dioxide in Aqueous Medium. *Colloid J.* **2001**, *63*, 253.
- (29) Salaices, M.; Serrano, B.; de Lasa, H. I. Experimental Evaluation of Photon Absorption in an Aqueous TiO<sub>2</sub> Slurry Reactor. *Chem. Eng. J.* **2002**, *90*, 219.
- (30) Toepfer, B.; Gora, A.; Li Puma, G. Photocatalytic Oxidation of Multicomponent Solutions of Herbicides: Reaction Kinetics Analysis with Explicit Photon Absorption Effects. *Appl. Catal., B* **2006**, *68*, 171.
- (31) Martín, C. A.; Baltanás, M. A.; Cassano, A. E. Photocatalytic Reactors I. Optical Behavior of Titanium Oxide Particulate Suspensions. *J. Photochem. Photobiol., A* **1993**, *76*, 199.
- (32) Cabrera, M. I.; Alfano, O. M.; Cassano, A. E. Absorption and Scattering Coefficients of Titanium Dioxide Particulate Suspensions in Water. *J. Phys. Chem.* **1996**, *100*, 20043.
- (33) Palmisano, L.; Augugliaro, V.; Camprostrini, R.; Schiavello, M. A Proposal for the Quantitative Assessment of Heterogeneous Photocatalytic Processes. *J. Catal.* **1993**, *143*, 149.
- (34) Serpone, N.; Terzian, R.; Lawless, D.; Kennepohl, P.; Sauve, G. On the Usage of Turnover Numbers and Quantum Yields in Heterogeneous Photocatalysis. *J. Photochem. Photobiol., A* **1993**, *73*, 11.
- (35) Ollis, D. F. Kinetics of Liquid Phase Photocatalyzed Reactions: An Illuminating Approach. *J. Phys. Chem. B* **2005**, *109*, 2439.
- (36) Minero, C.; Vione, D. A Quantitative Evaluation of the Photocatalytic Performance of TiO<sub>2</sub> Slurries. *Appl. Catal., B* **2006**, *67*, 257.
- (37) Murzin, D. Y. Heterogeneous Photocatalytic Kinetics: Beyond the Adsorption/Desorption Equilibrium Concept. *React. Kinet. Catal. Lett.* **2006**, *89*, 277.
- (38) Murzin, D.; Salmi, T. *Catalytic Kinetics*; Elsevier: Amsterdam, 2005.
- (39) Augugliaro, V.; Palmisano, L.; Minero, C.; Pelizzetti, E. Photocatalytic Degradation of Phenol in Aqueous Titanium Dioxide Dispersions. *Toxicol. Environ. Chem.* **1988**, *16*, 89.
- (40) Chen, D.; Ray, A. K. Photocatalytic Kinetics of Phenol and its Derivatives over UV Irradiated TiO<sub>2</sub>. *Appl. Catal., B* **1999**, *23*, 143.
- (41) Salaices, M.; Serrano, B.; de Lasa, H. I. Photocatalytic Conversion of Phenolic Compounds in Slurry Reactors. *Chem. Eng. Sci.* **2004**, *59*, 3.
- (42) Brandi, R. J.; Citroni, M. A.; Alfano, O. M.; Cassano, A. E. Absolute Quantum Yields in Photocatalytic Slurry Reactors. *Chem. Eng. Sci.* **2003**, *58*, 979.

Received for review February 5, 2007  
 Revised manuscript received March 27, 2007  
 Accepted March 30, 2007

IE070205H